J Am Soc Nephrol 13: 1721–1732, 2002

Expression of Hypoxia-Inducible Factor-1α and -2α in Hypoxic and Ischemic Rat Kidneys

CHRISTIAN ROSENBERGER,*† STEFANO MANDRIOTA,‡ JAN STEFFEN JÜRGENSEN,* MICHAEL S. WIESENER,* JAN H. HÖRSTRUP,* ULRICH FREI,* PETER J. RATCLIFFE,‡ PATRICK H. MAXWELL,‡ SEBASTIAN BACHMANN,† and KAI-UWE ECKARDT*

*Departments of *Nephrology and Medical Intensive Care and †Anatomy, Charité, Humboldt University, Berlin, Germany, and ‡Welcome Trust Centre for Human Genetics, Oxford, United Kingdom.*

Abstract. Oxygen tensions in the kidney are heterogeneous, and their changes presumably play an important role in renal physiologic and pathophysiologic processes. A family of hypoxia-inducible transcription factors (HIF) have been identified as mediators of transcriptional responses to hypoxia, which include the regulation of erythropoietin, metabolic adaptation, vascular tone, and neoangiogenesis. *In vitro*, the oxygen-regulated subunits HIF-1α and -2α are expressed in inverse relationship to oxygen tensions in every cell line investigated to date. The characteristics and functional significance of the HIF response *in vivo* are largely unknown. High-amplification immunohistochemical analyses were used to study the expression of HIF-1α and -2α in kidneys of rats exposed to systemic hypoxia bleeding anemia, functional anemia (0.1% carbon monoxide), renal ischemia, or cobaltous chloride (which is known to mimic hypoxia). These treatments led to marked nuclear accumulation of HIF-1α and -2α in different renal cell populations. HIF-1α was mainly induced in tubular cells, including proximal segments with exposure to anemia/carbon monoxide, in distal segments with cobaltous chloride treatment, and in connecting tubules and collecting ducts with all stimuli. Staining for HIF-1α colocalized with inducible expression of the target genes heme oxygenase-1 and glucose transporter-1. HIF-2α was not expressed in tubular cells but was expressed in endothelial cells of a small subset of glomeruli and in peritubular endothelial cells and fibroblasts. The kidney demonstrates a marked potential for upregulation of HIF, but accumulation of HIF-1α and HIF-2α is selective with respect to cell type, kidney zone, and experimental conditions, with the expression patterns partly matching known oxygen profiles. The expression of HIF-2α in peritubular fibroblasts suggests a role in erythropoietin regulation.

Sufficient oxygenation is a prerequisite for organ function. However, oxygen delivery to organs and tissue oxygen tensions within organs vary considerably. The kidney is characterized by an interesting paradox with respect to its oxygen supply. Although blood flow is high in relation to organ weight and the arteriovenous oxygen difference is small, shunt diffusion of oxygen and heterogeneous utilization lead to marked oxygen gradients (1,2). Oxygen supply to the renal medulla barely exceeds demand, and medullary oxygen tensions are approximately 10 mmHg (3–6). Cortical oxygen tensions are more heterogeneous but are also frequently less than the venous oxygen tensions (4,6–8).

The effects of oxygen on cellular functions of the kidney are poorly understood. High rates of oxygen consumption in the proximal tubule and thick ascending limb, together with limited oxygen supply, are thought to be responsible for the high sensitivity to ischemic injury (2,9,10). A physiologic function directly related to renal oxygen tensions is the production of erythropoietin (EPO) by peritubular cortical fibroblasts (11–13). Regulation of EPO occurs at the mRNA level but, because of the lack of an appropriate *in vitro* system, the control of EPO gene expression in the kidney remains incompletely characterized. Studies of EPO regulation in hepatoma cells led to the identification of a family of hypoxia-inducible transcription factors (HIF) (14,15). In addition to EPO, the HIF system regulates several target genes that have important functions in renal physiologic and pathophysiologic processes, including energy metabolism [glucose transporters (GLUT) and glycolytic enzymes], vasomotor regulation [nitric oxide synthases, heme oxygenase-1 (HO-1), and endothelins], angiogenic growth (vascular endothelial growth factor and platelet-derived growth factor), matrix metabolism (collagens, collagen prolyl hydroxylases, matrix metalloproteinases, and transforming growth factor-β isoforms), and apoptosis/cell survival decisions (NIP3 and Nix) (14–16). Therefore, it might be predicted that an understanding of the patterns of HIF regulation in the kidney would provide important insights into processes mediated by these molecules.

HIF is a heterodimer composed of an α-subunit and a β-subunit. Although HIF-β is constitutively expressed, its two

Received January 29, 2002. Accepted March 7, 2002.
Correspondence to Dr. Kai-Uwe Eckardt, Department of Nephrology and Medical Intensive Care, Charité, Campus Virchow-Klinikum, Augustenburger Platz 1, 13353 Berlin, Germany. Phone: ++49-30-4505-53433; Fax: ++49-30-4505-53909; E-mail: kai-uwe.eckardt@charite.de

1046-6673/1307-1721
Journal of the American Society of Nephrology

DOI: 10.1097/01.ASN.0000017223.49823.2A

dimerization partners, HIF-1α and -2α, are rapidly degraded in the presence of oxygen, via the ubiquitin-proteasome system. The von Hippel-Lindau gene product is the recognition component of a multiprotein E3-ubiquitin-ligase complex that captures HIF α-chains that have undergone enzymatic hydroxylation of specific prolyl residues (17,18). The oxygen dependence of HIF prolyl hydroxylation results in HIF α-subunit accumulation during hypoxia. *In vitro*, virtually every cell line responds to hypoxia with increases in the levels of HIF-1α and -2α, as well as of HIF target genes, suggesting that HIF are ubiquitous effectors of cellular responses to hypoxia (19,20). When HeLa cells in suspension were exposed to progressive decreases in pericellular oxygen levels, continuous increases in HIF protein levels and DNA binding activity were observed, with half-maximal induction at 1.5 to 2% O_2 (21). This range corresponds to oxygen tensions of approximately 10 to 15 mmHg, which are well within the range of values observed in the renal medulla under baseline conditions and in other parts of the kidney during hypoxia.

To assess the potential roles of HIF-1α and -2α in the renal response to hypoxia, we studied the expression of both proteins in the kidneys of rats exposed to hypoxia, anemia, functional anemia induced by carbon monoxide (CO), total or subtotal ischemia, or cobaltous chloride ($CoCl_2$) (which is known to mimic hypoxic effects). Our data indicate that both HIF α-subunits are induced in the kidney under these conditions but their expression is restricted to distinct cell populations, with the patterns differing depending on the type of stimulus.

Materials and Methods

Animals

The study was approved by the institutional review board for the care of animal subjects and was performed in accordance with National Institutes of Health guidelines. Male Sprague-Dawley rats (Winkelmann, Borchen, Germany) were used at weights of 200 to 280 g ($n = 3$ to 5 for each time point and experimental condition).

Induction of Anemia

A femoral artery catheter was inserted under anesthesia, and the hematocrit level was decreased by repetitive blood drawing and substitution of normal saline solution for a period of 45 min, until a value of 0.16 was reached. Animals were allowed to regain consciousness and were euthanized after 3 h.

Exposure to Hypoxia and CO

An air-tight Plexiglas cabinet was used to expose animals to premixed gasses. For the induction of normobaric hypoxia, animals were exposed for 1 or 5 h to 8% O_2/92% N_2. For the induction of functional anemia, animals were exposed for 0.5, 1, or 5 h to normal air supplemented with 0.1% CO.

Treatment with $CoCl_2$

$CoCl_2$ hexahydrate was dissolved in distilled water and injected subcutaneously twice, at a dose of 30 mg/kg, with a dosing interval of 12 h. Animals were euthanized 6 h after the second injection.

Induction of Renal Ischemia

For induction of total renal ischemia, the left renal artery was clamped for 0.5 or 1 h after a midline laparotomy. In a separate group of animals, a branch of the left renal artery was ligated for 1 d, to induce renal infarction. In sham-operated animals, the left renal artery was dissected from the vein but not clamped. The abdomen was sutured, and the animals were allowed to regain consciousness until euthanasia.

Tissue Preparation

For collection of kidneys, animals received intraperitoneal injections of sodium pentobarbital (Sanofi, Hannover, Germany), at a dose of 0.05 g/kg. In experiments with exposure to low ambient O_2 levels or CO, animals were returned to the chamber after injection and the chamber was flushed with the respective gas mixture. After the onset of anesthesia, kidneys were generally perfusion-fixed *in situ*, as described (22). In brief, a polyethylene tube was inserted into the infrarenal aorta and the inferior vena cava was incised. Perfusion was performed with 330 mosmol/L sucrose in phosphate-buffered saline (PBS) for 10 s at a constant pressure of 240 mmHg, followed by freshly prepared 3% paraformaldehyde in PBS (pH 7.4) at 240 mmHg for 1.5 min and at 100 mmHg for 3.5 min and then by sucrose/PBS to stop fixation. Additional kidneys from animals euthanized by cervical dislocation were fixed by immersion. After fixation, specimens were transferred to 330 mosmol/L sucrose in PBS with 0.02% sodium azide; 1 to 7 d later, specimens were embedded in paraffin.

Immunohistochemical Analyses and Anti-HIF Antibody Characterization

Paraffin sections (4 μm) were dewaxed in xylene, rehydrated in a series of ethanol washes, and placed in distilled water before staining procedures. Slides were coated with 3-aminopropyl-tri-ethoxysylane. For detection of HIF isoforms, monoclonal mouse anti-human HIF-1α antibody (α67; Novus Biologicals, Littleton, CO) and polyclonal rabbit anti-mouse HIF-2α antibodies (PM8 and PM9, obtained from two different rabbits immunized with a peptide containing amino acids 337 to 439 of mouse HIF-2α) were used. Specific staining of each HIF α-isoform was confirmed in immunoblots (20) by using *in vitro* transcribed and translated mouse HIF-1α and HIF-2α (TnT T7; Promega, Madison, WI) and homogenates of rat endothelial cells (RBE 4; kindly provided by Hugo Marti, Zurich, Switzerland) exposed to hypoxia *in vitro* (1% oxygen, 4 h) (Figure 1). For immunohistochemical analyses, α67 was used at a dilution of 1:6000 and PM8 and PM9 were used at dilutions of 1:3000. Additional primary antibodies were anti-chicken calbindin D-28K (1:30,000; Sigma Chemical Co., St. Louis, MO) as a marker for connecting tubules (23), polyclonal rabbit anti-rat Tamm-Horsfall protein (1:3000; a gift from John Hoyer, Philadelphia, PA) as a marker for thick ascending limbs (24), polyclonal rabbit anti-mouse thiazide-sensitive cotransporter (1:6000; a gift from David H. Ellison, Denver, CO) as a marker for distal convoluted tubules (25), monoclonal mouse anti-rat CD31 (1:200; Serotec, Oxford, UK) for staining of endothelial cells, polyclonal rabbit anti-mouse HO-1 (1:60,000; Stressgen, Victoria, Canada), and polyclonal rabbit anti-human Glut-1 (1:10,000; Biotrend, Golden, CO). Detection of bound antibodies was performed by using biotinylated secondary anti-mouse or anti-rabbit antibodies and a catalyzed signal amplification system (Dako, Hamburg, Germany) based on the streptavidin-biotin-peroxidase reaction, according to the instructions provided by the manufacturer. Antigen retrieval was performed for 90 s in preheated Dako target retrieval solution, using a pressure cooker. All incubations were performed in a humidified chamber.

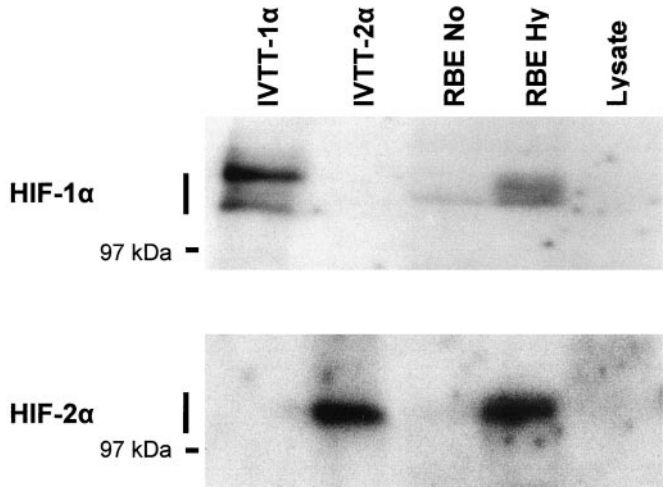

Figure 1. Antibody specificity of α67 [monoclonal mouse anti-human hypoxia-inducible transcription factor-1α (HIF-1α)] and PM9 (polyclonal rabbit anti-mouse HIF-2α). Immunoblots of *in vitro* transcribed and translated mouse HIF-1α (IVTT-1α) and HIF-2α (IVVT-2α) using reticulocyte lysates and homogenates of RBE cells under normoxic (No) and hypoxic (Hy) conditions, are presented. Lysate, unprogrammed reticulocyte lysates, used as negative control samples. Primary antibodies were diluted 1:1000 for immunoblotting.

Between incubations, specimens were washed two to four times in buffer (50 mM Tris-HCl, 300 mM NaCl, 0.1% Tween-20, pH 7.6). Control samples included samples from normoxic or sham-operated animals, samples prepared with the omission of primary antibodies, and samples prepared with the use of preimmune serum from animals immunized against HIF-2α.

Ultrastructural Preembedding Histochemical Analyses

With the use of a modified standard protocol (26), 15-μm sections were maintained in 2-ml glass vessels and subjected to the same procedures as the sections mounted on glass slides. Anti-mouse HIF-2α antibodies were diluted 1:1000 and incubation times were increased fourfold, compared with the protocol provided by the manufacturer (Dako). After staining, the sections were treated with 1.5% glutaraldehyde and 1% OsO_4, dehydrated with a graded ethanol series, and flat-embedded in Epon 812. Semithin sections were stained with Richardson's reagent, and additional ultrathin sections were processed for electron microscopy as described (26).

Signal Analysis

Signals were analyzed with a Leica DMRB microscope (Leica, Bensheim, Germany), using differential interference contrast. Photographs were digitally recorded by means of a Visitron system (Visitron, Puchheim, Germany).

Reagents

Unless otherwise indicated, chemicals were obtained from Sigma.

Results

Normoxia

In normoxic animals, immunohistochemical analyses for HIF-1α revealed no significant staining in the renal medulla or the cortex (Figure 2a and data not shown). Immunohistochemical analyses for HIF-2α occasionally demonstrated weak cytoplasmic staining of some tubular cells in the cortex and medulla and of medullary interstitial cells after prolonged reaction with diaminobenzidine. An identical weak staining pattern was observed with preimmune serum, however, and staining was thus considered to be nonspecific.

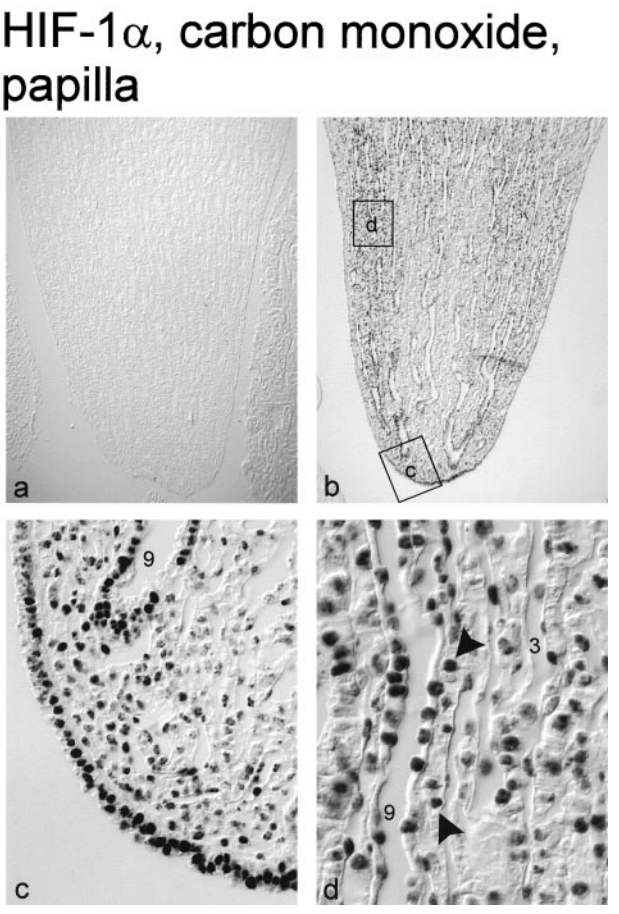

Figure 2. Expression of HIF-1α in the papilla of rats exposed to carbon monoxide (CO) for 5 h. (a) Normoxic control sample, showing no staining at baseline. (b) Sample showing marked upregulation after CO exposure. (c and d) Higher-magnification views of the areas of the papillary tip and middle papilla outlined in b. Arrowheads, interstitial fibroblasts. Magnifications: ×20 in a and b; 160 inc; and ×220 ind. 3, thin limb; 9, medullary collecting duct.

Normobaric Hypoxia

To activate the HIF system, we first exposed animals to 8% O_2 for 1 or 5 h. Irrespective of the mode of kidney fixation (immersion or perfusion), no signals for HIF-1α or -2α could be detected after 1 h. After 5 h, nuclear staining for HIF-1α was observed in cortical tubules, papillary collecting ducts, and papillary interstitial cells when kidneys were immersion-fixed (data not shown). Because of the lower morphologic resolution, compared with perfusion fixation, the identity and precise distribution of the positively staining cells were difficult to define. Because signals were not detectable after perfusion fixation, we hypothesized that the unavoidable reoxygenation

period of a few minutes might have been sufficient to allow HIF degradation. This assumption is based on experience with tissue cultures, in which the half-lives of HIF-1α and -2α after reoxygenation were observed to be only a few minutes (20,21).

Anemia and CO Exposure

Comparison of Stimuli. To overcome the potential loss of signal, animals were phlebotomized or exposed to CO to reduce their oxygen-carrying capacity and tissue oxygenation (27–30). Because of the much higher affinity of hemoglobin for CO, compared with O_2, exposure to 0.1% CO results in approximately 50% CO-hemoglobin; this effect slowly ceases when animals are returned to normal air. Acute anemia and CO exposure for 5 h resulted in pronounced and similar staining patterns for both HIF-1α and -2α, but CO exposure was a better tolerated and more reproducible stimulus. The signal intensity was slightly stronger after immersion fixation, but the signal distribution was independent of the mode of fixation. We therefore proceeded with perfusion-fixed kidneys from CO-exposed animals, to identify the cell types expressing HIF (Figures 2 to 6).

HIF-1α. Staining for HIF-1α after 5 h of CO exposure was observed in cell nuclei in both the cortex and medulla. The number and intensity of HIF-1α-positive cells varied in different zones of the kidney, with staining being most pronounced in the papilla. Within each zone, expression was restricted to subsets of cells (Table 1 and Figures 2 to 4).

In the cortex, HIF-1α was expressed only in tubular cells, with strongest expression in the S2 segment (Figure 3a). Slightly more than one-half of the S2 cross-sections were positive and, within each tubular cross-section, approximately one-half of the nuclei stained for HIF-1α. In S1 and S3 segments, only single cells stained positive. Distal tubular cells in the cortex were usually negative (Figure 3d), whereas connecting tubules and cortical collecting ducts regularly stained positive (Figure 3, a, b, and f). There was no overlap between staining for HIF-1α and that for Tamm-Horsfall protein (Figure 3, b and c) or the thiazide-sensitive cotransporter (Figure 3, d and e), but overlap was observed with counterstaining for the connecting tubule marker calbindin (Figure 3, f and g).

Within the deep cortex, signals consistently accumulated in the vicinity of arcuate veins (Figure 4a). In the outer stripe of the outer medulla, collecting ducts stained positive, whereas S3 segments of proximal tubules very rarely demonstrated signals and thick ascending limbs were negative. In the inner stripe, in addition to collecting duct cells, thick ascending limb segments and occasionally thin limbs were positive (Figure 4b). Cross-sections revealed that HIF staining increased with increasing distance from vascular bundles (Figure 4c).

In the deeper medulla, collecting ducts remained positive but, in contrast to other areas of the kidney, interstitial cells also expressed HIF-1α, with the proportion of positive cells increasing toward the tip of the papilla (Figure 2, b to d). Thin tube-like structures were also positive. On the basis of their hairpin appearance, some of those structures could be identified as thin limbs of the loop of Henle, but the possibility that some were capillaries, with endothelial cells expressing HIF-1α, cannot be excluded. Strong signals were also observed in papillary surface endothelial cells covering the papilla (Figure 2, b and c).

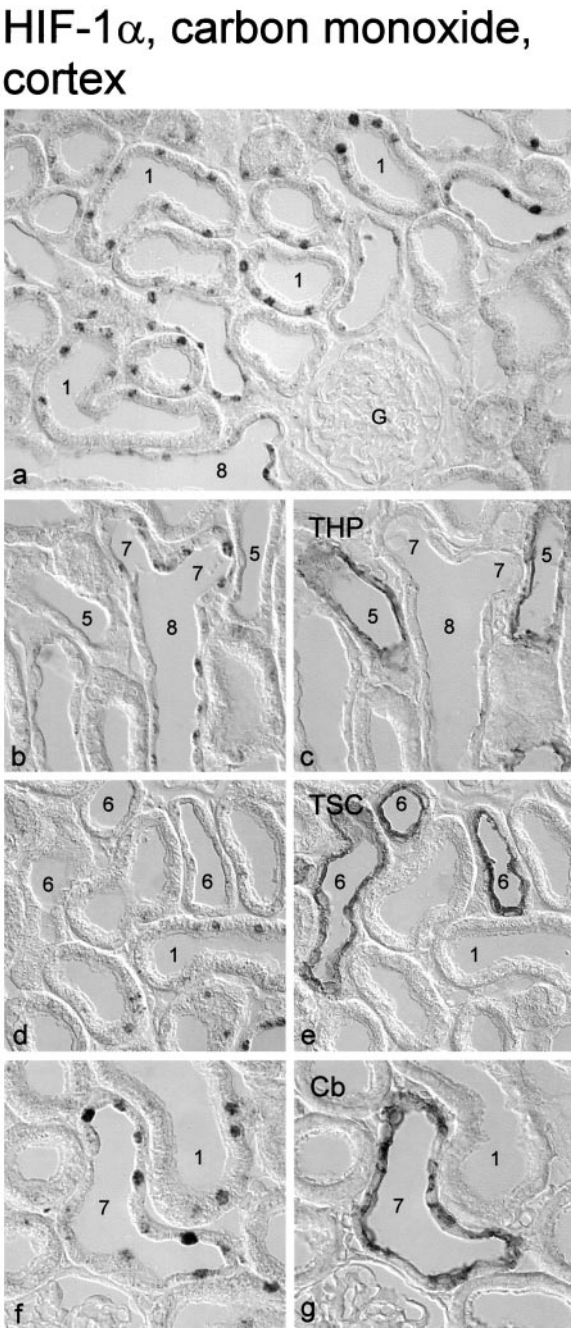

Figure 3. Expression of HIF-1α in the cortex of rats exposed to CO for 5 h. (b and c, d and e, and f and g) Pairs of serial sections of a medullary ray (b and c) and the cortical labyrinth (d to g) were stained for HIF-1α (b, d, and f) and markers used for identification of different nephron segments, namely Tamm-Horsfall protein (THP) for identification of the medullary thick ascending limb (c), thiazide-sensitive cotransporter (TSC) for identification of distal convoluted tubules (e), and calbindin D-28K (Cb) for identification of connecting tubules (g). 1, proximal tubule, pars convoluta; 5, cortical thick ascending limb; 6, distal convoluted tubule; 7, connecting tubule; 8, cortical collecting duct; G, glomerulus. Magnification, ×250.

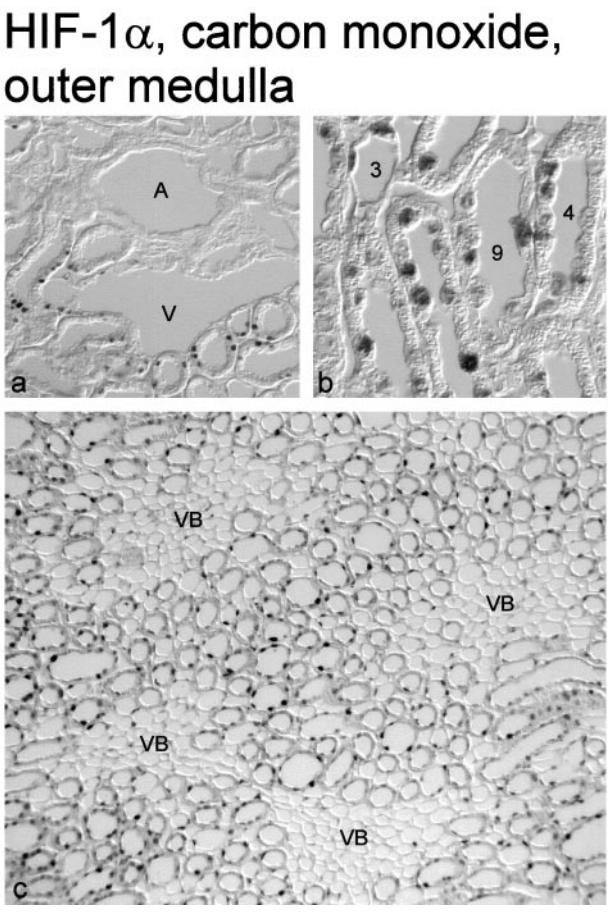

Figure 4. Expression of HIF-1α in the outer medulla of rats exposed to CO for 5 h. (a) Area at the corticomedullary border, showing preferential expression of HIF-1α in perivenous tissue. (b) Section of the inner stripe of the outer medulla, showing staining for HIF-1α in thin limbs, thick ascending limbs, and collecting ducts. (c) Cross-section of the inner stripe of the outer medulla, showing that HIF induction increases with increasing distance from vascular bundles (VB). 3, thin limb; 4, medullary thick ascending limb; 9, medullary collecting duct; A, arcuate artery; V, arcuate vein. Magnifications: ×120 in a, ×250 in b, ×80 in c.

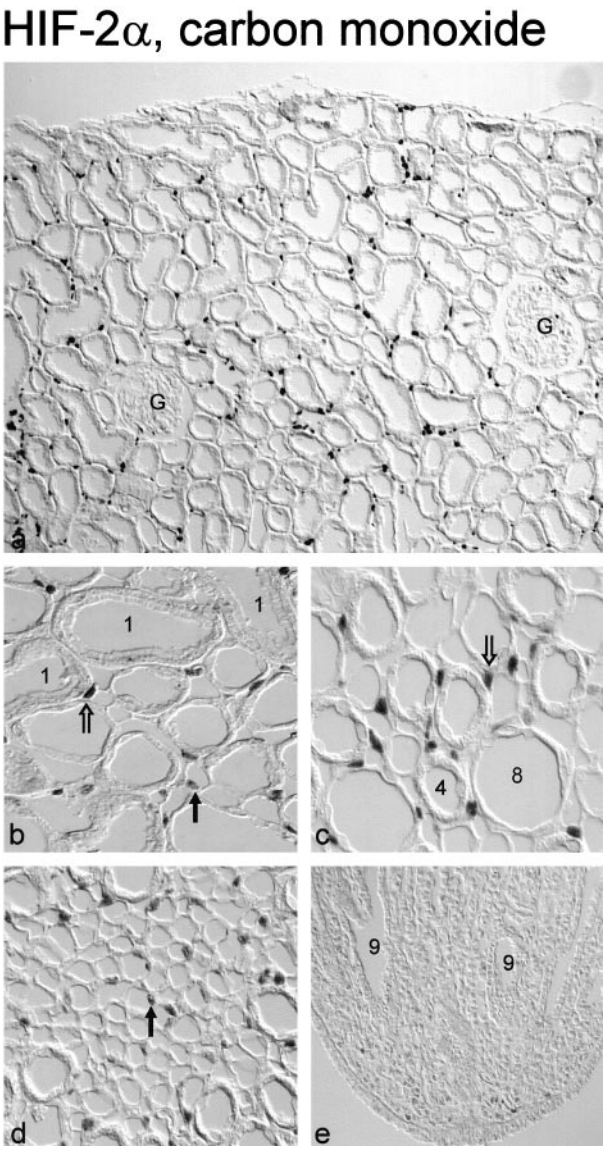

Figure 5. Expression of HIF-2α in kidneys of rats exposed to CO for 5 h. (a) Cortical labyrinth. (b) Outer stripe. (c and d) Inner stripe of the outer medulla. (e) Papilla. Peritubular cells in the cortex stain positive. In the outer medulla, both interstitial cells outside medullary rays (open arrows) and capillary endothelial cells within vascular bundles (black arrows) stain positive. 1, proximal tubule, pars convoluta; 4, medullary thick ascending limb; 8, cortical collecting duct; 9, medullary collecting duct; G, glomerulus. Magnifications: ×100 in a; ×220 in b, c, and d; ×120 in e.

HIF-2α. Staining for HIF-2α revealed an entirely different staining pattern, with virtually no overlap (Table 1 and Figure 5). HIF-2α was not detected in epithelial cells of any tubular segment, but some cells were stained in a small subgroup of glomeruli (<10%) (Figure 5a) and peritubular interstitial cells in the cortex and medulla frequently stained positive (Figure 5, b to d). In the inner stripe of the outer medulla, positive cells included some capillary endothelial cells of the vasa recta (Figure 5d). Overall, HIF-2α signal density decreased from the inner medulla toward the papillary tip, with the latter being virtually devoid of staining (Figure 5e). The staining patterns obtained with the two different antisera (PM8 and PM9) were identical.

To identify the glomerular and interstitial cell types staining for HIF-2α, we attempted double-labeling either for HIF-2α and CD31 (as a marker for endothelial cells) or for HIF-2α and 5'-ectonucleotidase (as a marker for peritubular fibroblasts) (22). Unfortunately, the anti-5'-ectonucleotidase antibody did not stain paraffin sections and the specimen heating required for HIF detection resulted in a loss of signal. Three other approaches were therefore pursued, *i.e.*, staining for HIF-2α and the endothelial antigen CD31 on consecutive sections and analysis of semithin sections by light microscopy and of ultrathin sections by electron microscopy after preembedding histochemical analysis. Labeling for HIF-2α and CD31 in the peritubular interstitium was only partially overlapping (Figure 6, a and b). This finding suggested that at least some of the

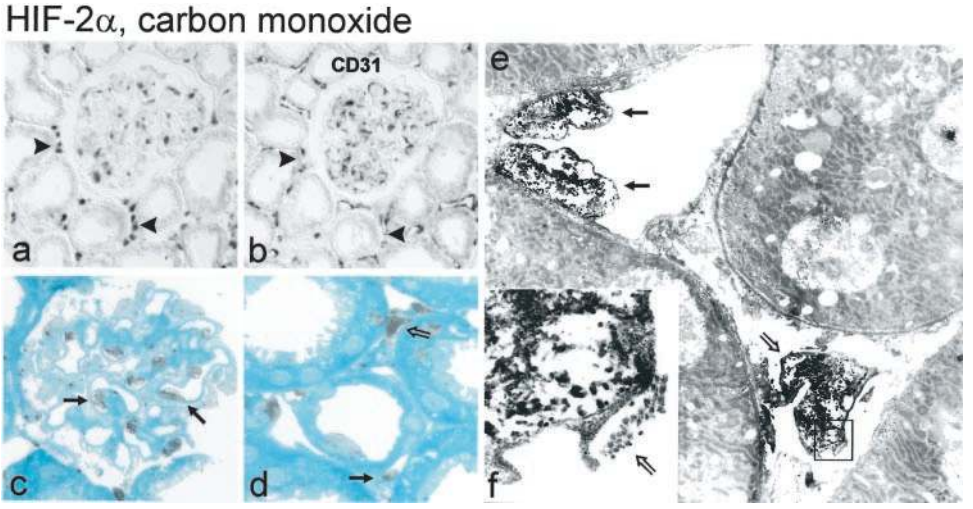

Figure 6. Evidence for expression of HIF-2α in glomerular and peritubular endothelial cells and peritubular fibroblasts. (a and b) Consecutive sections stained for HIF-2α (a) and the endothelial marker CD31 (b). Arrowheads, corresponding regions. HIF-2α-positive cells sometimes appear in clusters, with the number exceeding the possible number of peritubular endothelial cells. Conversely, some peritubular capillaries are clearly distant from HIF-2α-positive cells in the same area. (c and d) Semithin sections showing HIF-2α staining in glomerular endothelial cells (c, arrows), peritubular endothelial cells (d, black arrow), and peritubular fibroblasts (d, open arrow). (e) Transmission electron-microscopic views of the peritubular space, showing staining for HIF-2α in both peritubular endothelial cells (black arrows) and peritubular fibroblasts (open arrow). (f) Higher-magnification view of the area outlined in e, showing collagen bundles as a characteristic of fibroblasts (open arrow). Magnifications: ×250 in a and b; ×400 in c and d; ×4000 in e; ×20,000 in f.

cells expressing HIF-2α were nonendothelial, because they seemed to be located either outside capillaries or in clusters surrounded by smaller numbers of CD31-positive cells. Semithin sections demonstrated that nuclear staining for HIF-2α occurred in glomerular and peritubular endothelial cells and in peritubular interstitial cells that, on the basis of their location and triangular shape, seemed to be peritubular fibroblasts (Figure 6, c and d). This observation was confirmed by electron microscopy (Figure 6, e and f), which demonstrated positive nuclei of endothelial cells bulging into capillary lumina and of fibroblasts located between tubules and capillaries.

Study of animals after 0.5 or 1 h of CO exposure revealed that the HIF-1α signal commenced in the papilla and subsequently reached the collecting ducts and the cortical labyrinth. With increasing stimulation time, both the numbers of cells staining positive for HIF-1α and -2α and the signal intensity increased (data not shown).

$CoCl_2$

The induction patterns for HIF-1α and -2α with $CoCl_2$ stimulation were similar to the patterns with CO stimulation, insofar as HIF-1α was primarily induced in tubular cells and in interstitial cells in the inner medulla (Figure 7), whereas HIF-2α occurred in peritubular and some glomerular cells only (Table 1). However, tubular distribution for HIF-1α in response to $CoCl_2$ differed markedly from that observed in response to CO. Proximal tubular cells were negative, and marked induction of HIF-1α was observed in 70 to 80% of distal tubular cross-sections (Figure 7, a to c). In further contrast to CO exposure, there was no predominance of perivenous upregulation of HIF-1α in the deep cortex (Figure 7d). Moreover, collecting ducts of the lower papilla were negative in animals treated with $CoCl_2$ (Figure 7e).

Renal Ischemia

HIF-1α. Total renal ischemia also induced HIF-1α and -2α, and the staining patterns for both subunits were similar, although not identical, to those observed with CO. In the cortex, ischemia induced HIF-1α in some cells in a small number of glomeruli (Figure 8b). As with CO stimulation, connecting tubules and collecting ducts, but not proximal tubules, appeared positive (Figure 8, a and c). However, because perfusion was less effective, the morphologic resolution was lower and the possibility that some of the tubular signals were derived from cells other than those of connecting tubules or collecting ducts cannot be excluded with certainty. Total ischemia also induced HIF-1α in papillary tubular and interstitial cells (Figure 8, d to f). Staining in the papilla was not homogeneous. Staining began in a band in the outermost zone beneath the papillary surface (Figure 8d) and proceeded toward more central areas (Figure 8e). One day after the induction of renal infarction via ligation of one branch of the renal artery, marked upregulation of HIF-1α was observed in a band of cells in the direct vicinity of necrotic tissue (Figure 8, g and h).

HIF-2α. The HIF-2α induction pattern observed after renal artery clamping was similar to those observed in response to the other two stimuli investigated. However, staining seemed to occur more frequently in glomeruli and in endothelial cells, including the vasa recta of the outer stripe and

Table 1. Summary of HIF-1α and -2α expression patterns[a]

	HIF-1α			HIF-2α		
	Carbon Monoxide	Cobaltous Chloride	Total Ischemia	Carbon Monoxide	Cobaltous Chloride	Total Ischemia
Cortex						
glomeruli	−	−	+ (r)	++ (<10%)	+ (<10%)	+ (<10%)
S1	++ (r)	−	−[b]	−	−	−
S2	+++	−	−[b]	−	−	−
S3	+ (r)	−	−[b]	−	−	−
TAL	−	−	−[b]	−	−	−
macula densa	−	−	−[b]	−	−	−
DCT	−	++	−[b]	−	−	−
CNT	++	+++	++	−	−	−
CD	++	++	++	−	−	−
IC	−	−	−	+++	+	+
EC	−	−	−	++	+	+
Outer stripe						
S3	++ (r)	−	−[b]	−	−	−
TAL	−	−	−[b]	−	−	−
CD	++	++	++	−	−	−
IC	−	−	−	++	+	+[c]
EC	−	−	−	+	+ (r)	+[c]
Inner stripe						
thin limbs	+ (r)	+ (r)	−	−	−	−
TAL	++	+	−	−	−	−
CD	+++	+++	++	−	−	−
IC	+ (r)	−	−	+++	+	+
EC	−	−	−	+	+	+
Inner medulla						
CD	++	+ (r)	−	−	−	−
IC	++	++	−	+++	−	−
thin limbs/EC	++ (r)	++	−	+++	−	−
Papilla						
CD	+++	−	+++	−	−	−
IC	+++	+++	+++	−	−	−
thin limbs/EC	++	+++	+	−	−	−

[a] HIF, hypoxia-inducible factor; S1 to S3, proximal tubule segments; TAL, thick ascending limb; DCT, distal convoluted tubule; CNT, connecting tubule; CD, collecting duct; IC, interstitial cells; EC, endothelial cells. The average signal intensity for each cell type within the different zones of the kidney is indicated as follows: −, no staining; +, weak but definite staining; ++, strong staining; +++, very strong staining; r, staining of the respective cell type was observed only rarely and not in every specimen obtained under a certain condition; <10%, overall <10% of glomeruli stained positive.

[b] Because of inhomogeneous perfusion fixation after renal artery clamping, the overall resolution of tissue morphologic features was lower and identification of tubular structures was less certain; therefore, staining of some tubular segments that overall appeared negative cannot be excluded with certainty.

[c] Under ischemic conditions, it was not possible to clearly attribute signals in the outer stripe to interstitial or endothelial cells.

periglomerular arterioles (Table 1). Signal distribution and intensity were not different in immersion-fixed kidneys.

Comparison of HIF-1α Staining with Target Gene Expression

To test for the functional significance of HIF induction in tubular cells, consecutive tissue sections were stained for HIF-1α and two different target genes that have the potential to attenuate hypoxic injury and are known to be inducible by HIF *in vitro*, *i.e.*, HO-1 and GLUT-1 (31,32). HO-1 expression was not observed with normoxia (data not shown) but increased markedly in the proximal tubules of animals exposed to CO; the expression pattern colocalized with that for HIF induction. The cells with the most pronounced nuclear staining for HIF-1α frequently demonstrated the strongest expression of HO-1 (Figure 9, a and b). Expression of GLUT-1 under normoxic conditions was confined to the distal tubules and collecting ducts, as described previously (33) (data not shown).

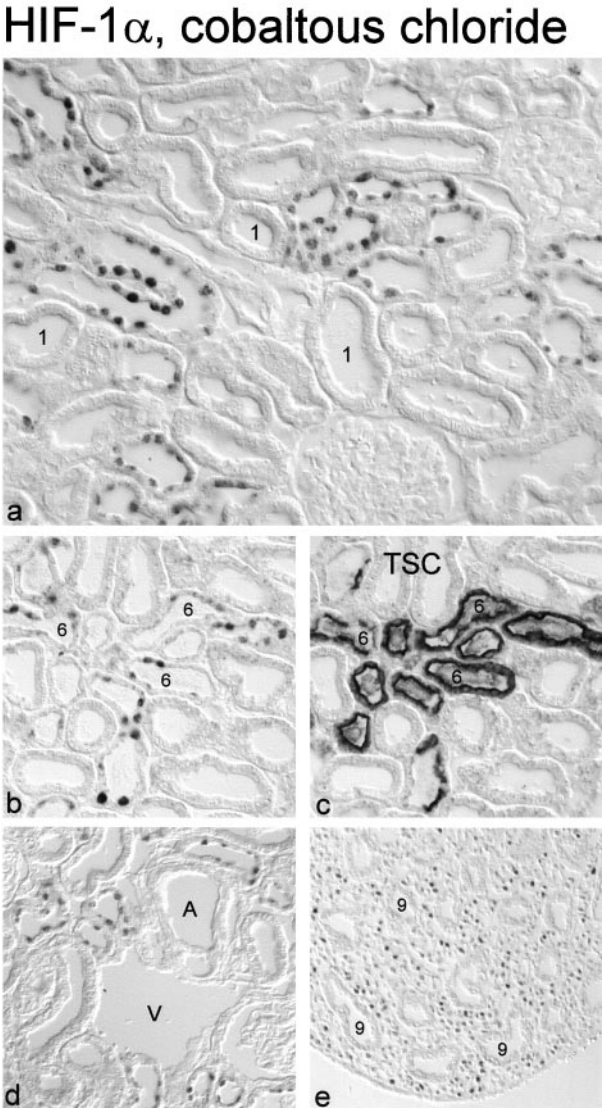

Figure 7. Expression of HIF-1α in the cortical labyrinth (a to c), the deep cortex (d), and the papillary tip (e) in rats treated with $CoCl_2$. (c) Consecutive section of b, stained for the thiazide-sensitive cotransporter (TSC) for identification of distal convoluted tubules. It should be noted that, in contrast to CO stimulation (Figure 3, d and e), HIF-1α expression is colocalized with thiazide-sensitive cotransporter expression. Staining of the deep cortex (d) shows no preferential expression around arcuate veins, as observed with CO stimulation (compare with Figure 4a). 1, proximal tubule, pars convoluta; 6, distal convoluted tubule; 9, medullary collecting duct; A, arcuate artery; V, arcuate vein. Magnifications: ×250 in a; ×200 in b and c; ×120 in d; ×160 in e.

During hypoxia, GLUT-1 expression was also strongly upregulated in proximal tubules expressing HIF-1α (Figure 9, c and d).

Discussion

This work is the first analysis in the kidney and the first comparative study of the cellular expression of the two oxygen-regulated subunits, 1α and 2α, of HIF with different stimuli *in vivo*. It demonstrates that the system is operative in the kidney and that both subunits are inducible. For specific detection of the two isoforms in immunohistochemical analyses, a potent signal amplification system was used. Nevertheless, no signals were observed in animals maintained with ambient oxygen tensions, despite the well known heterogeneity of renal oxygen tensions (3–6,8). Marked upregulation occurred, however, in nuclei of restricted renal cell populations under all conditions of systemic or local hypoxia investigated, indicating very specific, rather than widespread, activation of HIF, with a considerable amplitude of modulation.

The selective expression of HIF-1α and -2α seems to reflect a combination of intrinsic cellular capabilities and microenvironmental stimulation. Clear discrimination between the two factors is inevitably difficult, but several observations support a dominant role for either intrinsic or extrinsic factors in certain cells and under certain conditions. The most striking observation indicating the involvement of intrinsic determinants was that, independent of the type of stimulus, the cell populations expressing HIF-1α and -2α were consistently different. Whereas HIF-1α was predominantly expressed in tubular cells, HIF-2α expression was largely confined to cells within the peritubular interstitium (Figures 2 to 8). This finding suggests that the vast majority of cells that respond with HIF activation under certain conditions express only one of the two isoforms, indicating an important difference between the *in vivo* situation and regulation in cell lines (which usually demonstrate hypoxic induction of both isoforms) (20). The expression of HIF-2α in glomerular and peritubular endothelial cells confirms that this isoform plays a predominant role in the hypoxic adaptation of endothelial cells, which was postulated when the protein was identified and termed "endothelial PAS" protein (34). However, in agreement with subsequent *in vitro* work (20), our findings indicate that HIF-2α is not an endothelium-specific transcription factor. Cumulative evidence from the staining of consecutive sections with an endothelial marker and fine-structural analyses clearly demonstrated additional staining of peritubular fibroblasts (Figure 6).

Another observation indicating a specific cellular predisposition for HIF activation was the predominant expression of HIF-1α in connecting tubules and collecting ducts. Irrespective of known differences in local oxygen tensions in the cortex and medulla, collecting duct cells were positive in all zones of the kidney, independent of the type of stimulation (Figures 2, c and d, 3, a and b, 4b, and 8, c and f). This induction was highly selective, because other nephron segments in the immediate vicinity were usually negative. The mechanism of this preferential expression remains unclear, but upregulation in ischemic kidneys suggests that it does not essentially depend on urine flow and regular transport activity.

Other structures and cell populations demonstrated nuclear accumulation of HIF only in certain locations and only under some conditions investigated, which suggests that local determinants were more important for those responses. In glomeruli, for example, HIF-1α was not induced in response to anemia or CO but was induced after renal artery clamping (Figures 3a and 8b). This finding could indicate that, under conditions in which

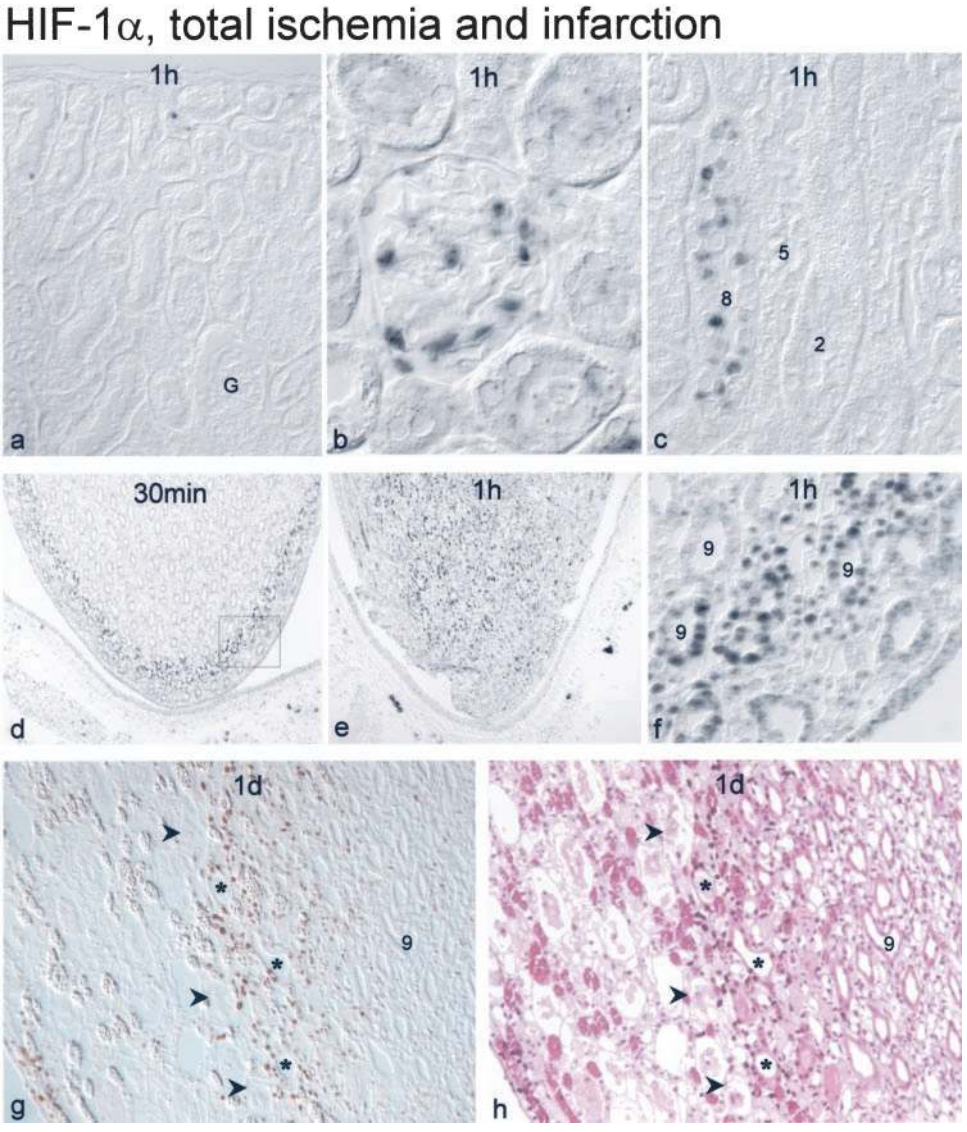

Figure 8. HIF-1α expression in kidneys rendered ischemic by renal artery occlusion for 30 min (d) or 60 min (a to c, e, and f) or renal artery branch ligation for 24 h (g and h). A few tubular cells (a) and some glomeruli (b) in the cortical labyrinth and collecting ducts in the medullary rays (c) stain positive. In the papilla (d to f), expression can be observed in collecting ducts and interstitial cells, starting in superficial areas at 30 min and progressing toward the center after 1 h. (f) Higher-magnification view of the area outlined in d. In infarcted kidneys, HIF-1α expression can be observed in cells located adjacent to necrotic tissue (arrowheads) (g and h show the same section stained for HIF-1α before and after counterstaining with hematoxylin and eosin). 2, proximal tubule, pars recta; 5, cortical thick ascending limb; 8, cortical collecting duct; 9, medullary collecting duct; G, glomerulus. Magnifications: $\times$250 in a, c, and f; $\times$450 in b; $\times$60 in d and e; $\times$150 in g and h.

arterial oxygen tension was normal, local oxygen tensions in glomeruli might not have been sufficiently low for HIF-1α induction. Stimulus-dependent activation of the HIF system was also observed in many tubular cell types. Upregulation of HIF-1α in distal convoluted tubules in response to $CoCl_2$, for example (Figure 7b), is presumably related to local uptake and accumulation (35,36). In support of this assumption, selective apical uptake of cobalt, presumably via a carrier-mediated influx process, was demonstrated in the distal tubule-derived MDCK cell line (37). After exposure to CO, activation in particular tubular segments often seemed to be in keeping with oxygen gradients. A perivenous distribution of positively staining tubules was observed near the corticomedullary junction (Figure 4a), and HIF expression in the inner medulla increased with increasing distance from vascular bundles (Figure 4c). Within the thick ascending limb, positive cells were more commonly observed in the inner stripe, compared with the outer stripe, of the outer medulla (Figure 4b), which corresponds to an established gradient of hypoxia sensitivity (2). Further evidence for local oxygen gradients determining HIF induction was obtained after renal infarction, with staining occurring at the border of tissue necrosis throughout different kidney zones (Figure 8, g and h).

However, consideration of different nephron segments also suggests that the hypoxic thresholds for HIF activation vary widely among different cell types. Within proximal tubules, for

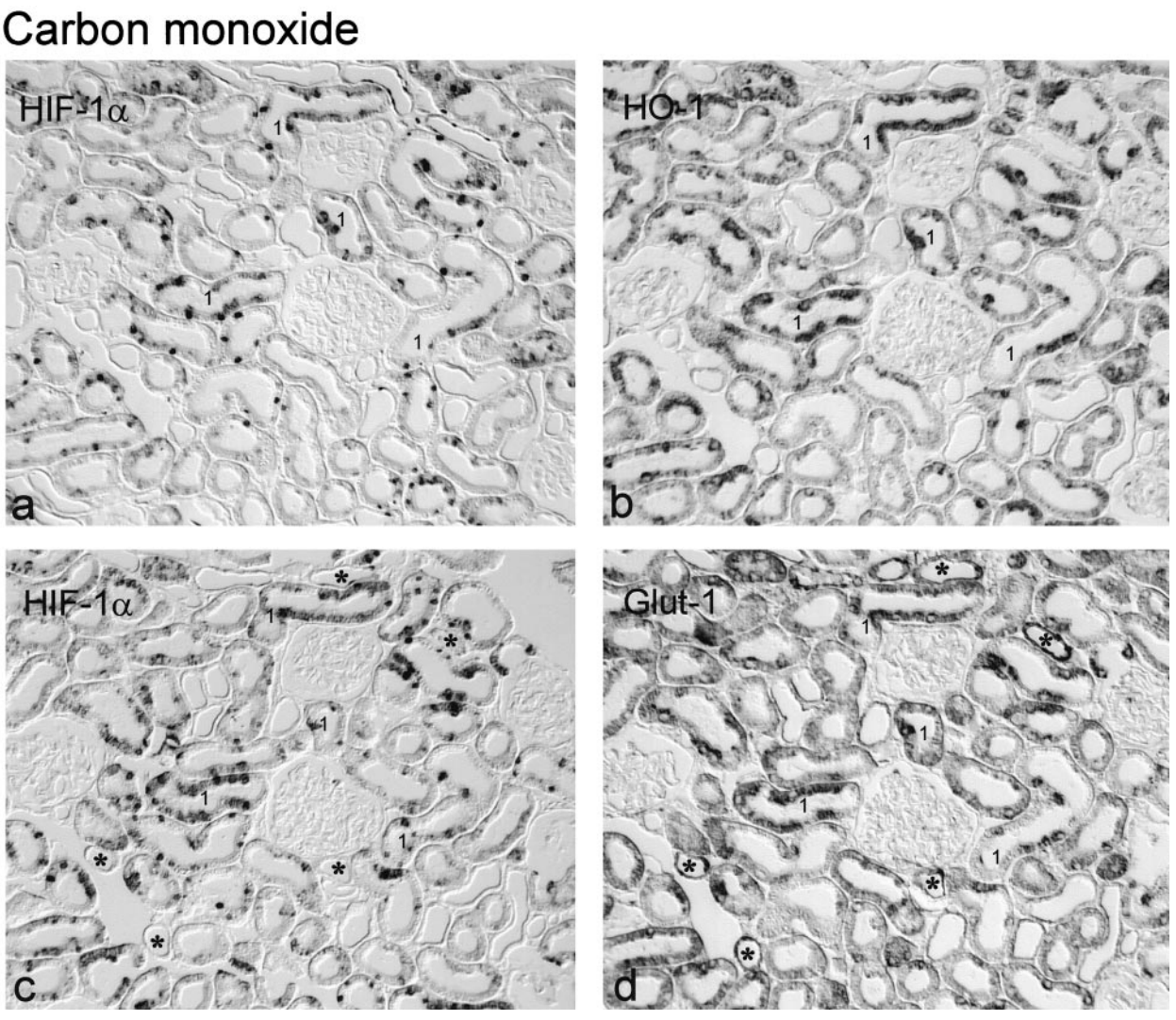

Figure 9. HIF-1α expression and staining for heme oxygenase-1 (HO-1) and glucose transporter-1 (GLUT-1) in two pairs of consecutive sections (a/b and c/d) from the renal cortex. Sections were processed such that adjacent surfaces were stained and "mirrored" after digital recording ("back-to-back" processing). The almost complete overlap between tubular cells expressing HIF-1α and HO-1 or GLUT-1 should be noted. GLUT-1 expression in distal tubules not expressing HIF-1 (stars) was constitutive and not different from that in normoxic animals. Magnification, ×150.

example, upregulation of HIF-1α was much more frequent in the convoluted part (S1 and S2 segments) than in the straight part (S3 segment), although, because of local oxygen gradients, straight rather than convoluted proximal tubules are more sensitive to hypoxic injury (9,38,39). Although cobalt strongly induced HIF-1α in distal convoluted tubules, CO stimulation seemed insufficient to induce HIF-1α in these segments, even when adjacent proximal tubules and collecting ducts were positive. Furthermore, the normally hypoxic papillae did not stain positive in unstimulated animals, despite the fact that normal papillary oxygen tension values are probably lower than those achieved in the cortex of stimulated animals. Given the low basal level, papillary oxygen tensions are thought to exhibit little further reduction in response to reduced renal oxygen supply (3–6). Nevertheless, strong upregulation of HIF-1α was inducible in papillary tubular and interstitial cells. Therefore, it seems likely that the cell type determines not only the ability to express one or the other HIF α-isoform but also the level of hypoxia at which the system is activated.

Irrespective of the reasons for selective induction of HIF-1α and -2α in different parts of the kidney, the specific immunohistochemical procedures developed in this study provide powerful tools for elucidation of HIF function *in vivo*, including differences in HIF-1- *versus* HIF-2-dependent target gene activation. The most well defined oxygen-dependent function of the kidney is the production of EPO (41), and we previously identified peritubular cortical fibroblasts as the cellular sites of hormone production (12,13). Three of the experimental conditions used in this investigation, *i.e.*, anemia, CO, and $CoCl_2$, strongly induce EPO mRNA in the kidney, whereas renal ischemia is only a weak stimulus for EPO production (42). Parallelism with the expression of HIF-2α in cortical peritubular cells, as observed in this study,

indicates a role for HIF-2α in EPO regulation. In contrast, for two other hypoxia-inducible genes (HO-1 and GLUT-1) (31,43), we observed clear colocalization with HIF-1α expression in distinctive tubular cells (Figure 9). This colocalization also provides a strong indication that HIF protein, as demonstrated in this study by means of immunohistochemical analysis, is transcriptionally active and mediates physiologically relevant adaptation.

Although HIF expression was restricted to certain cell populations under each condition investigated, it is remarkable that the majority of renal cell types were observed to express one of the two isoforms under at least one of the conditions (Table 1). This indicates a widespread capability for altered gene expression in the kidney in response to hypoxia. There is increasing consideration of the role that hypoxia might play not only in acute renal failure but also in the progression of chronic renal disease (44). However, establishing a link between altered cell biologic processes and renal tissue oxygen profiles remains difficult. Studies of HIF expression in renal pathologic conditions, in comparison with the patterns established in this study, could prove useful in providing further insight into the role of hypoxia in the progression of renal lesions. Given the fact that HIF is a key regulator of genes that mediate adaptation to hypoxia, it is tempting to speculate that the level of HIF induction not only indicates cellular hypoxia but also modulates the extent of hypoxic injury.

Acknowledgments

Drs. Rosenberger and Mandriota contributed equally to this work. Financial support was provided by the German Research Foundation (Grant EC 87-3) and a Marie Curie individual fellowship to Dr. Mandriota.

References

1. Lübbers DW, Baumgärtl H: Heterogeneities and profiles of oxygen pressure in brain and kidney examples of pO_2 distribution in the living tissue. *Kidney Int* 51: 372–380, 1997
2. Epstein FH: Oxygen and renal metabolism. *Kidney Int* 51: 381–385, 1997
3. Kovacs G, Akhtar M, Beckwith BJ, Bugert P, Cooper CS, Delahunt B, Eble JN, Fleming S, Ljungberg B, Medeiros LJ, Moch H, Reuter VE, Ritz E, Roos G, Schmidt D, Srigley JR, Storkel S, van den BE, Zbar B: The Heidelberg classification of renal cell tumours. *J Pathol* 183: 131–133, 1997
4. Leichtweiss HP, Lübbers DW, Weiss C, Baumgärtl H, Reschke W: The oxygen supply of the rat kidneys: Measurements of intrarenal pO_2. *Pflügers Arch* 309: 328–349, 1969
5. Baumgärtl H, Leichtweiss HP, Lübbers DW, Weiss C, Hurland H: The oxygen supply of the dog kidney: Measurements of intrarenal pO_2. *Microvasc Res* 4: 247–257, 1972
6. Günther H, Aumüller G, Kunke S, Vaupel P, Thews G: The oxygen supply of the kidney. I. Distribution of O_2 partial pressures in the rat kidney under normal conditions. *Res Exp Med (Berl)* 163: 251–264, 1974
7. Schurek HJ, Jost U, Baumgärtl H, Bertram H, Heckmann U: Evidence for a preglomerular oxygen diffusion shunt in rat renal cortex. *Am J Physiol* 259: F910–F915, 1990
8. Welch WJ, Baumgärtl H, Lübbers D, Wilcox CS: Nephron pO_2 and renal oxygen usage in the hypertensive rat kidney. *Kidney Int* 59: 230–237, 2001
9. Ratcliffe PJ, Endre ZH, Scheinman SJ, Tange JD, Ledingham JG, Radda GK: ^{31}P nuclear magnetic resonance study of steady-state adenosine 5'-triphosphate levels during graded hypoxia in the isolated perfused rat kidney. *Clin Sci* 74: 437–448, 1988
10. Brezis M, Rosen S, Silvio P, Epstein FH: Selective vulnerability of the medullary thick ascending limb to anoxia in the isolated perfused rat kidney. *J Clin Invest* 73: 182–190, 1984
11. Jelkmann W: Erythropoietin: Structure, control of production, and function. *Physiol Rev* 72: 449–489, 1992
12. Bachmann S, Le Hir M, Eckardt K-U: Colocalization of erythropoietin mRNA and ecto-5'-nucleotidase immunoreactivity in peritubular cells of rat renal cortex indicates that fibroblasts produce erythropoietin. *J Histochem Cytochem* 41: 335–341, 1993
13. Maxwell PH, Osmond MK, Pugh CW, Heryet A, Nicholls LG, Tan CC, Doe BG, Ferguson DJ, Johnson MH, Ratcliffe PJ: Identification of the renal erythropoietin-producing cells using transgenic mice. *Kidney Int* 44: 1149–1162, 1993
14. Semenza GL: Regulation of mammalian O_2 homeostasis by hypoxia-inducible factor 1. *Annu Rev Cell Dev Biol* 15: 551–578, 1999
15. Pugh CW, Chang GW, Cockman M, Epstein AC, Gleadle JM, Maxwell PH, Nicholls LG, O'Rourke JF, Ratcliffe PJ, Raybould EC, Tian YM, Wiesener MS, Wood M, Wykoff CC, Yeates KM: Regulation of gene expression by oxygen levels in mammalian cells. *Adv Nephrol Necker Hosp* 29: 191–206, 1999
16. Sowter HM, Ratcliffe PJ, Watson P, Greenberg AH, Harris AL: HIF-1-dependent regulation of hypoxic induction of the cell death factors BNIP3 and NIX in human tumors. *Cancer Res* 61: 6669–6673, 2001
17. Ivan M, Kondo K, Yang H, Kim W, Valiando J, Ohh M, Salic A, Asara JM, Lane WS, Kaelin Jr WG: HIFα targeted for VHL-mediated destruction by proline hydroxylation: Implications for O_2 sensing. *Science (Washington DC)* 292: 464–468, 2001
18. Jaakkola P, Mole DR, Tian YM, Wilson MI, Gielbert J, Gaskell SJ, Kriegsheim AA, Hebestreit HF, Mukherji M, Schofield CJ, Maxwell PH, Pugh CW, Ratcliffe PJ: Targeting of HIF-α to the von Hippel-Lindau ubiquitylation complex by O_2-regulated prolyl hydroxylation. *Science (Washington DC)* 292: 468–472, 2001
19. Maxwell PH, Pugh CW, Ratcliffe PJ: Inducible operation of the erythropoietin 3' enhancer in multiple cell lines: Evidence for a widespread oxygen-sensing mechanism. *Proc Natl Acad Sci USA* 90: 2423–2427, 1993
20. Wiesener MS, Turley H, Allen WE, Willam C, Eckardt K-U, Talks KL, Wood SM, Gatter KC, Harris AL, Pugh CW, Ratcliffe PJ, Maxwell PH: Induction of endothelial PAS domain protein-1 by hypoxia: Characterization and comparison with hypoxia-inducible factor-1α. *Blood* 92: 2260–2268, 1998
21. Jiang BH, Semenza GL, Bauer C, Marti HH: Hypoxia-inducible factor 1 levels vary exponentially over a physiologically relevant range of O_2 tension. *Am J Physiol* 271: C1172–C1180, 1996
22. Dawson TP, Gandhi R, Le Hir M, Kaissling B: Ecto-5'-nucleotidase: Localization in rat kidney by light microscopic histochemical and immunohistochemical methods. *J Histochem Cytochem* 37: 39–47, 1989
23. Bindels RJ, Hartog A, Timmermans JA, van Os CH: Immunocytochemical localization of calbindin-D28k, calbindin-D9k and parvalbumin in rat kidney. *Contrib Nephrol* 91: 7–13, 1991

24. Sikri KL, Foster CL, MacHugh N, Marshall RD: Localization of Tamm-Horsfall glycoprotein in the human kidney using immuno-fluorescence and immuno-electron microscopical techniques. *J Anat* 132: 597–605, 1981
25. Obermuller N, Bernstein P, Velazquez H, Reilly R, Moser D, Ellison DH, Bachmann S: Expression of the thiazide-sensitive Na-Cl cotransporter in rat and human kidney. *Am J Physiol* 269: F900–F910, 1995
26. Bachmann S, Bosse HM, Mundel P: Topography of nitric oxide synthesis by localizing constitutive NO synthases in mammalian kidney. *Am J Physiol* 268: F885–F898, 1995
27. Jelkmann W, Seidl J: Dependence of erythropoietin production on blood oxygen affinity and hemoglobin concentration in rats. *Biomed Biochim Acta* 46: S304–S308, 1987
28. Eckardt KU, Ratcliffe PJ, Tan CC, Bauer C, Kurtz A: Age-dependent expression of the erythropoietin gene in rat liver and kidneys. *J Clin Invest* 89: 753–760, 1992
29. Sandner P, Wolf K, Bergmaier U, Gess B, Kurtz A: Hypoxia and cobalt stimulate vascular endothelial growth factor receptor gene expression in rats. *Pfluegers Arch* 433: 803–808, 1997
30. Hofbauer KH, Jensen BL, Kurtz A, Sandner P: Tissue hypoxygenation activates the adrenomedullin system *in vivo*. *Am J Physiol* 278: R513–R519, 2000
31. Semenza GL: HIF-1 and human disease: One highly involved factor. *Genes Dev* 14: 1983–1991, 2000
32. Agarwal A, Nick HS: Renal response to tissue injury: Lessons from heme oxygenase-1 gene ablation and expression. *J Am Soc Nephrol* 11: 965–973, 2000
33. Heilig C, Zaloga C, Lee M, Zhao X, Riser B, Brosius F, Cortes P: Immunogold localization of high-affinity glucose transporter isoforms in normal rat kidney. *Lab Invest* 73: 674–684, 1995
34. Tian H, McKnight SL, Russell DW: Endothelial PAS domain protein 1 (EPAS1), a transcription factor selectively expressed in endothelial cells. *Genes Dev* 11: 72–82, 1997
35. Quamme GA: Renal magnesium handling: New insights in understanding old problems. *Kidney Int* 52: 1180–1195, 1997
36. Hoenderop JG, Willems PH, Bindels RJ: Toward a comprehensive molecular model of active calcium reabsorption. *Am J Physiol* 278: F352–F360, 2000
37. Nagao M, Sugaru E, Kambe T, Sasaki R: Unidirectional transport from apical to basolateral compartment of cobalt ion in polarized Madin-Darby canine kidney cells. *Biochem Biophys Res Commun* 257: 289–294, 1999
38. Schurek HJ, Kriz W: Morphological and functional evidence for oxygen deficiency in the isolated perfused rat kidney. *Lab Invest* 53: 145–155, 1985
39. Shanley PF, Brezis M, Spokes K, Silva P, Epstein FH, Rosen S: Transport-dependent cell injury in the S3 segment of the proximal tubule. *Kidney Int* 29: 1033–1037, 1986
40. Deleted in proof.
41. Eckardt K-U: Erythropoietin: Oxygen-dependent control of erythropoiesis and its failure in renal disease. *Nephron* 67: 7–23, 1994
42. Pagel H, Jelkmann W, Weiss C: A comparison of the effects of renal artery constriction and anemia on the production of erythropoietin. *Pfluegers Arch* 413: 62–66, 1988
43. Fine LG, Bandyopadhay D, Norman JT: Is there a common mechanism for the progression of different types of renal diseases other than proteinuria? Toward the unifying theme of chronic hypoxia. *Kidney Int* 75: S22–S26, 1997
44. Norman JT, Clark IM, Garcia PL: Hypoxia promotes fibrogenesis in human renal fibroblasts. *Kidney Int* 58: 2351–2366, 2000

See related editorial, "The Breathing Kidney," on pages 1974–1976.